4-2016

Distribution of Shell Formation Proteins in Oyster Hemolymph, Hemocytes, and Mantle Tissue

Donald Joseph Kleppel

Follow this and additional works at: https://ecommons.udayton.edu/uhp_theses

 Part of the Biology Commons

Distribution of Shell Formation Proteins in Oyster Hemolymph, Hemocytes, and Mantle Tissue

Honors Thesis

Donald Joseph Kleppel

Department: Biology

Advisors: Karolyn Hansen, Ph.D. and Douglas Hansen, Ph.D.

April 2016

Distribution of Shell Formation Proteins in Oyster Hemolymph, Hemocytes, and Mantle Tissue

Honors Thesis
Donald Joseph Kleppel
Department: Biology
Advisors: Karolyn Hansen, Ph.D. and Douglas Hansen, Ph.D.
April 2016

Abstract

The occurrence and composition of L,3-4-dihydroxyphenylalanine-containing proteins (L-DOPA proteins) that participate in oyster shell formation has not been fully determined. It is known that the oyster mantle tissue is primarily responsible for shell formation and recent research has demonstrated the involvement of the hemolymph (blood) and hemocytes (blood cells). L-DOPA proteins are known to aid in the cross linking of shell formation proteins, in turn creating the insoluble organic matrix formed to produce the organic component of the shell. Using the biomarker amino acid L-DOPA, this research focuses on determining the localization of these shell formation proteins in hemocytes, hemolymph, and mantle tissue of *Crassostrea virginica* (the Eastern oyster). In order to study the localization of these proteins, rapid shell formation/repair will be induced by notching the oyster (mimicking predation) and shell protein composition and location will be determined as the oyster repairs the shell. Proteins responsible for shell formation and regeneration containing L-DOPA will be collected from the adductor muscle near the site of notching in the oysters. These proteins will be further examined after centrifugation by amino acid analysis of the cell pellet (hemocytes), supernatant (hemolymph), and mantle tissue rinsed in filtered sea water. The newly regenerated shell, like the other samples, will be extracted and analyzed for protein composition and distribution as well. All samples will be extracted at regular intervals beginning at time of induction and continuously throughout shell regeneration (t=0hrs, 48hrs, 96hrs, 168hrs, 2 weeks, 3 weeks, 4 weeks) in order to determine their amino acid composition. Amino acid analysis will be done using integrated pulse amperometry-anion exchange high performance liquid chromatography.

UNIVERSITY *of*
DAYTON

Table of Contents

Introduction:

Crassostrea virginica, the Eastern oyster, has been shown to regenerate its shell using biomineralization strategies. Many of the proteins that are crucial in shell formation include proteins containing the amino acid dihydroxyphenylalanine (L-DOPA) and other highly phosphorylated proteins (Wheeler 1992). L-DOPA proteins have been shown to play a role in the enzymatic cross linking of shell proteins to form the insoluble organic matrix (Bonucci 1992). However, much is unknown about the origin, distribution, concentration, and composition of these proteins in oyster shell formation. Therefore, the goal of this research is to specifically target and analyze L-DOPA proteins to determine their origin, distribution, concentration, and composition to reveal their possible role in shell formation. Previous research has indicated the role and composition of multiple molluscan shell matrix proteins along with soluble matrix molecules that have been shown to have activity in orienting calcium crystals as well as in *in vitro* nucleation (Gotliv et al. 2003, Zhang et al. 2006). Thus far, preliminary data indicate that L-DOPA proteins are being used in shell regeneration and we believe that these proteins can be found in the hemocytes, hemolymph, and mantle tissue, and are readily available for extraction and analysis. After decades of research, Carriker et al. 1980, came to find that the insoluble L-DOPA proteins most likely play a significant role in oyster shell formation by providing a scaffold for soluble matrix proteins to grow on. Once the presence of L-DOPA was detected by Wheeler at al. 1988, it was only a matter of time before scientists discovered the sclerotization (cross-linking) capabilities of L-DOPA and how this made it an excellent candidate for creating an insoluble protein matrix (Waite and Anderson 1978, Waite 1992).

The oyster shells are composed of 95-99% inorganic material (Kennedy et al. 1996), with the organic portion consisting of soluble and insoluble proteins that are cross linked (Wheeler et al. 1988). A more detailed view of these layers can be seen to the right in Figure 1. The two functions that are presumed
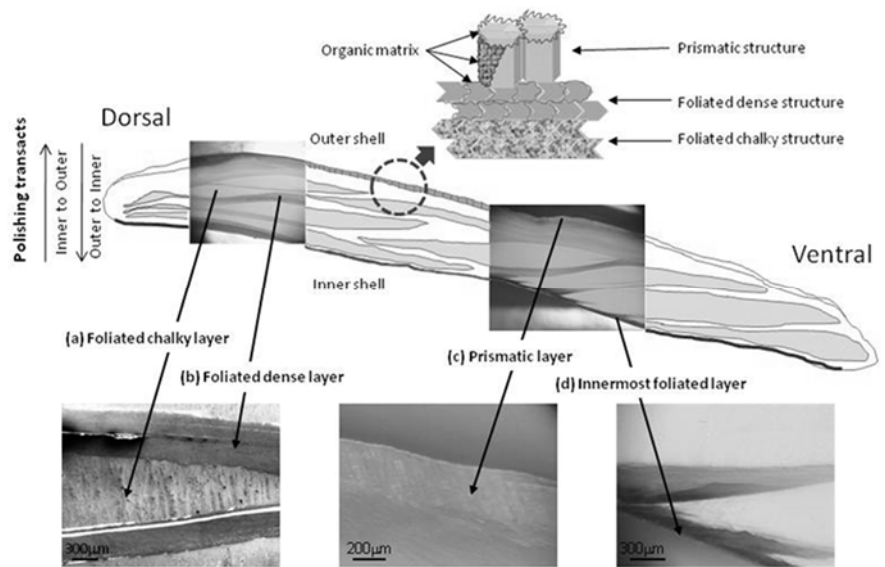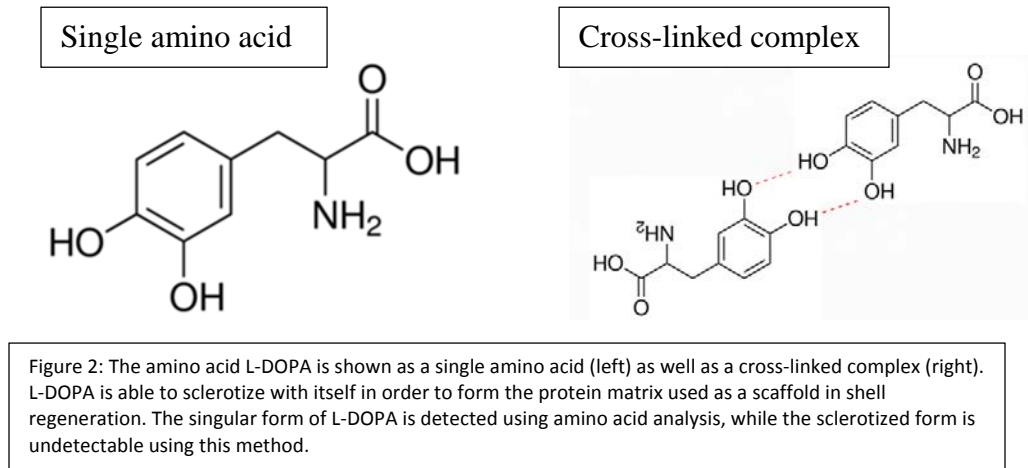

Figure 1: Depicts the different layers of oyster shell as shell is formed during growth and/or repair. Underneath the densely deposited outer shell lies the organic prismatic structure of interest. This layer acts as a protein scaffold, allowing foliated, dense structures to be deposited above it.

to come from this organic matrix have to do with crystal growth and a framework that will distribute fractional stresses (Smith et al. 1999). The function of the matrix is to assemble and align calcium carbonate crystals and has been studied and confirmed by multiple research groups (Zhang et al. 2006). The presence of L-DOPA proteins has been found in many different shelled species such as *Crassostrea gigas*, the Pacific oyster, and in oyster mantle tissue as well (Almeida et al 1998). L-DOPA proteins are not able to be detected at later stages of shell repair and are considered insoluble due to their ability to cross link, but they can be seen earlier on in repaired shell and are present in the mantle tissue. Figure 2 shows L-DOPA as a single amino acid (more easily detected by amino acid analysis) as well as a self-cross-linked complex that is one of the possible cross-linking mechanisms that would be present post-sclerotization.

Figure 2: The amino acid L-DOPA is shown as a single amino acid (left) as well as a cross-linked complex (right). L-DOPA is able to sclerotize with itself in order to form the protein matrix used as a scaffold in shell regeneration. The singular form of L-DOPA is detected using amino acid analysis, while the sclerotized form is undetectable using this method.

Hemocytes (blood cells) are mobile cells and can be considered potential transporters of L-DOPA to the site of shell formation and repair. Analysis of hemocytes and hemolymph will enable us to see if L-DOPA is being transported in the vasculature and in what quantities. Mantle tissue analysis will show the composition of L-DOPA in protein structures on the newly formed shell. In these analyses, a better understanding of the origin and composition of L-DOPA proteins will be obtained. In our laboratory, preliminary data indicated that L-DOPA proteins can be detected in the mantle tissue, hemocytes, and hemolymph of oysters (Hansen and Hansen 2013).

The first specific aim of this research was to measure the occurrence of L-DOPA content in oyster hemolymph, hemocytes, mantle tissue, and newly formed shells. In order to get an accurate representation of where L-DOPA proteins occur, we took samples from all these areas mentioned. Because these protein precursors are not well known in terms of their composition and location, we aimed to detect their presence in multiple target areas that are associated with shell regeneration in the oysters. This research enabled us to see the exact composition of these precursors and gave a better

shell mineralization model showing how the precursors can be transported by the cells in the oysters to the area of regeneration.

The other aim of this research was to observe if there was a change in L-DOPA composition as the oyster shell formed following a notching (shell damage) event. In order to see when and how the L-DOPA precursor proteins are deposited at the site of notch repair, we analyzed L-DOPA in the oyster and the newly formed repair shell matrix at different time points following notching. We hypothesized that newly formed shell in its earliest stages following notching will contain the greatest amount of L-DOPA and would gradually decrease as the shell was further mineralized and the proteins cross link to form the organic matrix/mineral ceramic outer coating. Rationale for this hypothesis came from the fact that L-DOPA proteins are not able to be detected in a highly cross linked state due to the alteration in composition that occurs during the cross linking process (when bonds are formed between residues to create the insoluble matrix). We have considered that the L-DOPA will not begin to cross link until later in the mineralization process and can be detected more so at early stages (before cross linking) than later stages (after cross linking).

Thus far, our research has focused on the hemolymph of oysters throughout the regeneration process. Of the 254 samples collected for processing in total, experiments and analysis of 21 samples of hemolymph at 0 hr, 48 hr, 96 hr, 168 hr, 2 weeks, 3 weeks, and 4 weeks has occurred. To recap on anticipated results, we expected to see relatively high levels of L-DOPA proteins present during the formation/repair of the shell, especially at the beginning of the regeneration response. As the regeneration process continues, less and less L-DOPA content would be seen due to the sclerotization of the

proteins to form an insoluble matrix. L-DOPA proteins would most likely be concentrated at the site of new shell formation throughout the regeneration.

This research is relevant to multiple fields as it will provide insight into how organic matrix assembly and wound repair occurs in the shells of mollusks. With a better understanding of the order and organization of bio-ceramic materials, this research will provide a model for composite ceramic growth and has applications in many fields including biology, biotechnology, nanotechnology, biomedical and corrosion engineering, biosynthetic implantation, etc. (Hansen and Hansen 2013). This research may have more specific applications in bone regeneration and in creating better interfaces for prosthetic devices. With apparent global warming events leading to ocean acidification, this research can also provide a better insight into shell regeneration for many different mineralized species that are exposed to changing environments (i.e. change in pH of water).

Materials & Methods:

In order to successfully analyze these proteins and get an accurate representation of their composition, additional specific experiments were conducted. Oyster were purchased from Pemaquid Oyster Company, Waldeboro, ME and maintained at 64°F in saltwater tanks in Kettering Labs (KLA-1). These tanks were connected to a mechanical, biological, and UV light filter system. Two sample populations of oysters were part of this experiment. One group of oysters was not notched, otherwise known as the *naïve* oysters, and the other group consisted of the notched oysters, or the *induced* oysters. Notching was performed using a tile saw to create a V shape on the edge of the oyster shell. We expected to see higher levels of L-DOPA proteins in the induced oysters after notching because notching is representative of a predation event where L-DOPA will be responsible for the regeneration processes to occur. Naïve oysters were notched immediately before harvesting of hemolymph, hemocytes, and mantle tissue (no chance for induction).

Hemocytes and hemolymph were analyzed after hemolymph was extracted. The hemocytes and hemolymph were harvested using a 22 gauge syringe that was placed in the adductor muscle of the oyster. Approximately 1.0 ml of the hemolymph was extracted at each
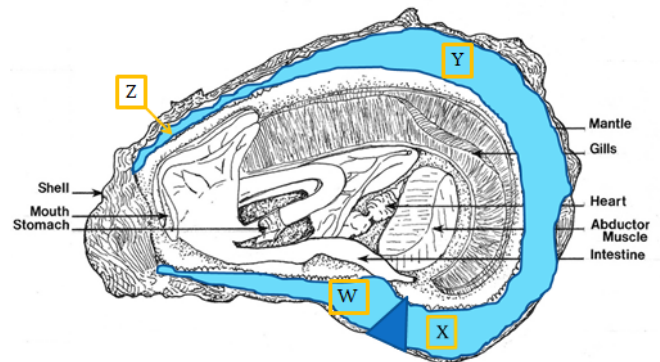
Figure 3: Inside anatomy of an oyster with representations of the notch (deep blue triangle), mantle tissue (light blue shading), and pieces of mantle sampled (orange squares – W, X, Y, Z).

sampling period in each oyster. Figure 3 (right), shows where the adductor muscle is located relative to the site of notching (represented by the deep blue triangle).

Centrifugation was used to separate the hemocytes from the hemolymph and the L-DOPA proteins were purified and analyzed for amino acid composition. Mantle tissue was cut using a standard razor blade sterilized with ethyl alcohol. Mantle samples were approximately 2 square centimeters and were taken from multiple margins of the organism. Figure 3 shows more specifically where these samples of mantle tissue were taken from during collection. Since processing did not happen immediately after collection, the tissue samples were stored at -80°C and analyzed at a later time. The newly formed shells of the induced oysters were collected to later be analyzed for L-DOPA residues. We hypothesized that there would be a larger number of granulocytes (a sub-class of hemocytes) carrying crystals in the hemolymph in the induced oyster group compared to the naïve group. We also believed that the majority of the crystals would be located in the hemocytes (more so than the supernatant of the hemolymph) in the induced group after collection and analysis when compared to the composition in the naïve group.

In order to accomplish the second aim of this research, samples of the newly formed shell were extracted and analyzed for their L-DOPA concentration and composition at different time points. Samples of hemocytes and hemolymph were extracted from 5 of the 32 oysters notched using a 22 gauge syringe immediately after notching took place (time 0). Samples were separated by centrifugation and stored at -80°C as previously stated. After 48 hours of repair, this process was repeated for 5 more oysters. After hemolymph and hemocyte samples were taken, the oysters were shucked open using a shucking knife and mantle tissue samples were taken as previously explained (4 mantle samples per oyster). This process was repeated at 96 hours, 168 hours, 2 weeks, 3 weeks, and 4 weeks. All samples were stored at -80°C until ready for

processing. More images of materials and methods used for experimentation can be seen at the end of this document (Appendices 4 and 5: PowerPoint slides presented at the Honors Student Symposium, March 2016, as well as Poster Presentation, National Shellfisheries Association Annual Meeting, February 2016, Las Vegas NV, USA).

All samples, after collection, were thawed and hydrolyzed for 17 hours at 110°C. 75 microliters of sample were transferred to 1.5 mL centrifuge tubes along with 100 microliters of 6M HCL and 10 microliters of phenol. The HCL evaporated until dry using a SpeedVac evaporator for approximately 4 hours. The samples were then regenerated in 300 microliters of deionized water and filtered. This regenerated hydrolysate underwent amino acid composition analysis using integrated amperometry. This was accomplished by injecting 25 microliters of diluted sample on a Dionex ICS3000 Amino Acid Analysis chromatography system that uses an electrochemical detector. A three point calibration was used to get the most accurate reading. In order to quantify the final amino acid composition these chromatography peaks were compared with NIST amino acid standards and water blanks. (Amino Acid Analysis Protocol was provided by Hansen laboratory protocol manual).

For protein hydrolysis and preparation for analysis, amino acid standard preparation, buffer preparation, and amino acid analyzer details, please see protocols in Appendices 1-3.

Results:

      Data analysis thus far has been done on 12 of the 21 samples of hemolymph

processed and put through amino acid analysis. These 12 samples were from the first 4

time points in sample collection (3 oysters sampled at 0 hr, 48 hr, 96 hr, and 168 hr). The

remaining data from the 9 samples that were processed (from the 2, 3, and 4 week time

points) has not yet been analyzed for amino acid concentration. Three samples (taken

from three separate oysters) during 0hr, 48 hr, 96 hr, 168 hr, 2 weeks, 3 weeks, and 4

weeks were processed. Also, samples were run on the amino acid analyzer 3 times each

in order to get a consistent and accurate representation of their contents. At 80 minutes

per run, this totals out at 84 hours of run time on the analyzer. Average picoMole

concentrations were taken from the three runs on each sample and from the three oysters

at each time point. Therefore, 9 separate items of concentration data from 9 different runs

at each time point were averaged to represent the final picoMole concentration for that

specific time point. At the 0 hr, 48 hr, 96 hr, and 168 hr time points, the average

picoMole concentrations were 0 pM, 159.1820 pM, 477.0401 pM, and 161.6811 pM

respectively. Just as the notching event occurred, at the 0 hr time point, samples were

taken, which showed to not produce a significant enough amount of L-DOPA for the

amino acid analyzer to detect. An increase in picoMole concentrations of L-DOPA were

then observed at the 48 hour sampling period. Again, an increase was observed at the 96

hr sampling period. At the 96 hr time point a peak in L-DOPA concentration was

observed. This time point was the most significant in terms of picoMole concentrations of

L-DOPA throughout the sampling period. After this, there was a decline in L-DOPA

concentrations in the hemolymph at the 168 hr point. All of these data are summarized in

Table 1 and Figure 4 shown below.

Table 1: Shows average mean, standard deviation, and %RSD of picoMole concentrations from the 0 hr, 48 hr, 96 hr, and 168 hr time points. These are the short term results (first week of processing). Highlighted in a red box is the 96 hr time point, the most significant in terms of L-DOPA concentrations in hemolymph in all samples processed and analyzed.

	Avg. Mean	Avg. stdev	Avg. %RSD
0hr -	0	0	0
48hr -	159.182	36.45395	49.61977
96hr -	477.0401	21.08499	3.9536
168hr -	161.6811	4.149533	2.632845

Concentration of L-DOPA in Week 1 Hemolymph
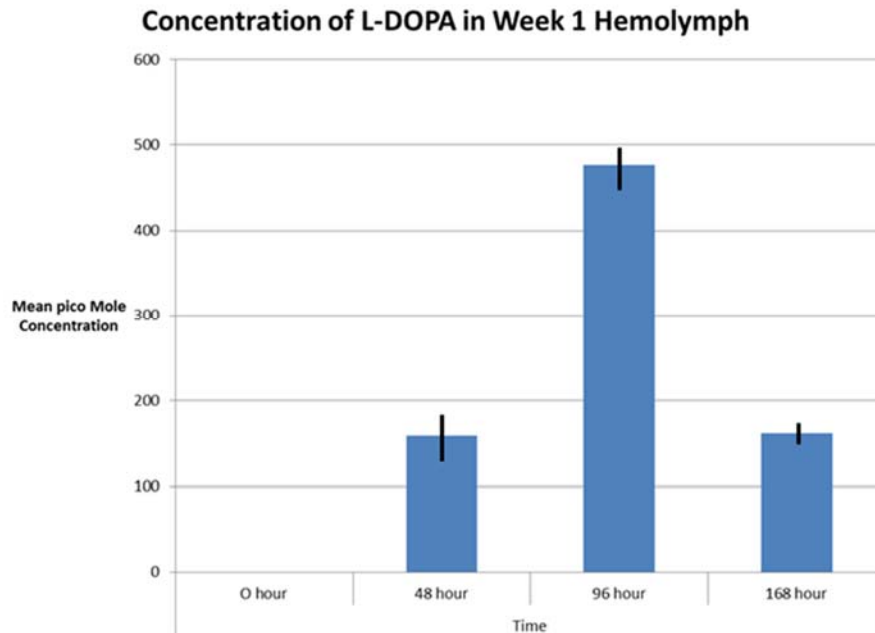
Figure 4: Bar graph representing the average mean and standard deviation of all samples processed at their respective time points. Summarizes the information provided in Table 1. A clear significant peak is observed at the 96 hr time point.

Chromatograph readings are another aspect of our results that allow visualization of the percent relative L-DOPA concentrations as compared to other amino acids present in sample. Standard chromatograph readings were taken from prepared standards (as explained in the Methods section) and from protocol taken from the National Institute of Standards and Technology (NIST). A standard chromatograph reading is shown in Figure 5-A. In Figure 5, the section of the chromatograph of particular interest is the one boxed and enlarged in blue. This section shows the L-DOPA peaks more closely. At the 0 hr chromatograph reading (Figure 5-B) there is no significant amount of L-DOPA detected, as is consistent with the average concentrations of L-DOPA presented previously in Table 1 and Figure 4. At the 48 hr time point, a slight rise in L-DOPA is observed (Figure 5-C). Figure 5-D shows the significant increase in L-DOPA as the largest peak observed from sample readouts on the chromatograph at the 96 hr time point. Figure 5-E shows a decline in L-DOPA concentration as represented by the slightly smaller peak on the chromatograph. Of the 9 chromatograph readings from each time point, the one most representative and consistent with the data provided in Table 1 was chosen for this paper. Figure 5 (Including frames A-E) and is shown on the following page.

Images of shell repair were taken with an 8 megapixel camera prior to notch, at 0 hr, 48 hr, 96 hr, 168 hr, and 12 weeks of repair. Images do not decipher details of prismatic shell structure, but rather show general shell deposits and macroscale changes in shell repair. Images can be seen in Figure 6 (Page 13).
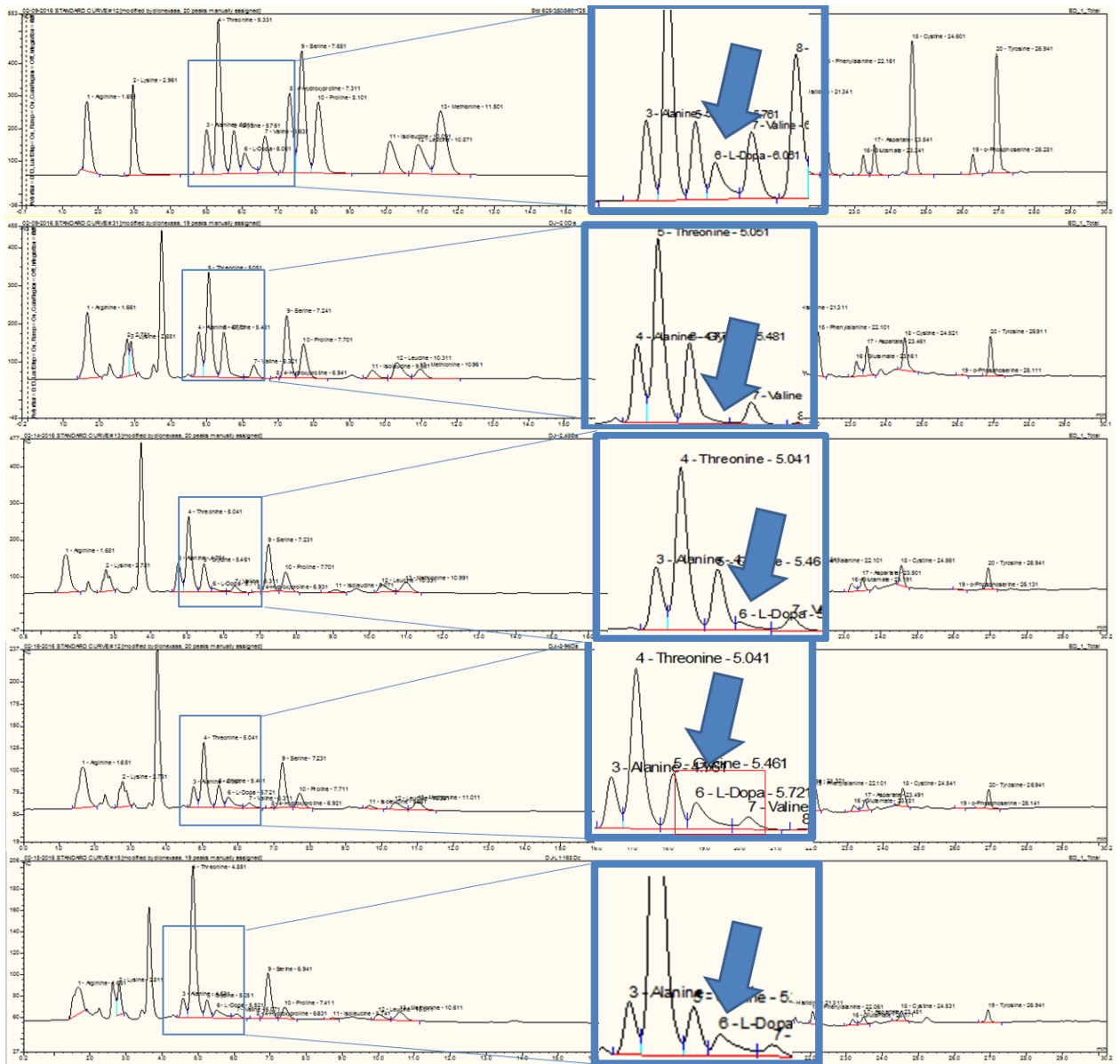
Figure 5: Chromatograph readings from NIST standards (Frame A) and sample readouts from the 0 hr, 48 hr, 96 hr, and 168 hr time points (Frames B-E) are shown. Each peak is labeled with the amino acid that it represents. L-DOPA peaks are enlarged for clarity in blue boxes to the right of the main peak readouts. Blue arrows point to the L-DOPA peaks. A red box highlights the L-DOPA peak at the most significant readout, the 96 hr time point.
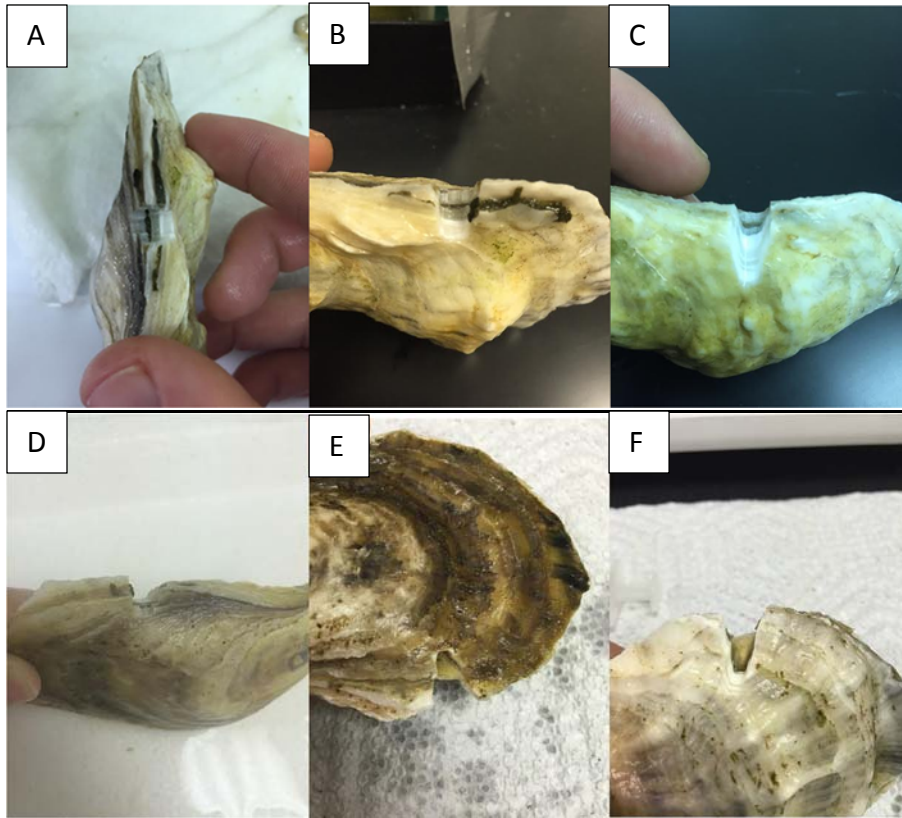
Figure 6: Images of shell during repair at 0 hr (A), 48 hr (B), 96 hr (C), 168 hr (D), 12 weeks (E & F). Small, transparent deposits can be seen in the first 168 hours, while significant, hard deposits can be observed 12 weeks after notching.

Discussion:

Thus far, analysis of the L-DOPA data in hemolymph suggests that L-DOPA proteins are being recruited to the site of repair following a notching event. Hemolymph is a good indicator of concentrations of L-DOPA following a notching event. However, a better understanding of concentrations of hemocyte L-DOPA content would allow for comprehension of the transport of these proteins as well. As previously hypothesized, we believed that L-DOPA proteins are being transported via hemocytes. L-DOPA found in hemolymph could result from the release of L-DOPA from lysed hemocytes following sample collection and before hemolymph/hemocyte separation via centrifugation. Data so far also suggests that there is a time frame in which L-DOPA resources are being recruited.

Further analyses of the results show that there is a slight delay in L-DOPA recruitment following a notching event. At the 0 hr mark, there was not a significant amount of L-DOPA detectable, as our calibration curve did not allow for detection of such small concentrations present in these samples. At the 48 hr mark, L-DOPA was in significantly higher concentrations in the hemolymph. 48 hours after this, at the 96 hr mark, L-DOPA concentrations reached a peak suggesting that although slightly delayed, the L-DOPA response does occur over a relatively quick time frame. After this 96 hr mark, there was a decline in L-DOPA as seen in the 168 hr time point. We hypothesized that resources would be allocated to the site of repair following the notching event, which did in fact occur. However, this time frame gives a more detailed description of when these resources are recruited. The decline in detected L-DOPA following the 96 hr peak most likely is due to the sclerotization process. Once L-DOPA, as a single amino acid, is

present in a high enough concentration (at the 96 hr time point) it will begin to sclerotize with itself and will no longer be detectable by amino acid analysis. From imaging, it was clear that an organic matrix was being deposited at the 96 hr and 168 hr time points. A decline in detected L-DOPA, therefore, can be explained by the cross-linked form of L-DOPA being undetectable by amino acid analysis even though L-DOPA is present at this time, possibly in higher concentrations than found at the 96 hr mark.

To get a better picture of not only the concentrations of L-DOPA in hemolymph over time, but also concentrations in hemocytes, mantle tissue, and newly regenerated shell, we will need to process the remaining 233 samples. We feel that, with the mantle tissue samples in particular, we will be able to get a much better understanding of the concentration gradient established by L-DOPA throughout the mantle of the oyster. With this new information, it will allow us to clarify if L-DOPA concentrations are rising in areas closer to the site of the shell (as hypothesized) or if the concentration of L-DOPA increases throughout the entire mantle. Given that the oyster has an open circulatory system, both hypotheses are plausible.

As previously mentioned in the Introduction section, this research is relevant for species that deposit mineralized shells. Specifically, with ocean acidification coinciding with global warming effects, this research can aid us in understanding more about the physiology of shell regeneration. Although the structure of the shell has been very well studied, the mechanisms for making the shell have not. Oysters, as well as other animals that deposit mineralized shells, will use a certain amount of resources and energy in shell generation. Future research can look into how much the energy budget changes in terms of allocating energy into shell formation after a predation event. Further investigations

may find that other functions, such as metabolism or reproductive mechanisms would be

impaired during a time of shell regeneration if organisms do indeed budget more energy

towards shell regeneration and take energy away from these less essential activities.

Future Direction:

In the future, we hope to continue with experiments involving the remaining samples of hemolymph, hemocytes, mantle tissue, and new shell to better determine how the oyster allocates protein resources for shell repair on a short time frame (immediate repair) and longer time frame (weeks after notch event). These data will provide us with insight into how the proteins are being transported, in what concentrations they are being used, and where these proteins are most prominent throughout the mantle during repair. As we previously predicted, we suspected that proteins would be transported via hemocytes to the notched area. We also suspected that they would be most concentrated in regions of mantle close to the sight of repair. In future studies, we hope to further explore these hypotheses.

Imaging of the repair sites is another important aspect of this research that we would like to further elaborate on. By using a high quality scanning electron microscope, better images of the oysters at various stages of repair could be taken. SEM images would allow for a better understanding of what repair looks like in the oysters, especially at early stages when it is particularly difficult to see the organic matrix layer being deposited. Overall, the bulk of the experiments conducted in the future will involve processing and analyzing the remaining samples and taking high quality images of shell repair.

Bibliography:

Almeida, M.J., J. Machado, M.A. Vieira Coelho, P. Soares da Silva, and J. Coimbra.
1998. L-3,4-Dihydroxyphenylalanine (L-DOPA) Secreted by Oyster
(*Crassostrea gigas*) Mantle Cells: Functional Aspects. *Comp. Biochem. Physiol.*
B 120:709-713

Bonucci, E. 1992. Calcification in Biological Systems. Boca Raton: CRC Press

Carriker, M.R., R.E. Palmer, and R.S. Prezant. 1980. Functional Ultramorphology
of the Dissoconch Valves of the Oyster *Crassostrea virginica*. *Proc. National*
Shellfisheries Association 70(2): 139-183.

Gotliv, B., L. Addadi, and S. Weiner. 2003. Mollusk Shell Acidic Proteins: In Search
of Individual Functions. *ChemBioChem* 4:522-529.

Hansen, K.M. and D.C. Hansen. 2013. "Role of Hemocytes in Molluscan Shell
Repair", Proposal to the National Science Foundation, Division of Molecular and
Cellular Biosciences.

Kennedy, V.J., R.I.E. Newell, and A.F. Eble. 1996. The Eastern Oyster *Crassostrea*
virginica. Maryland Sea Grant College Program, College Park, MD. 734 pp.

Smith, B.L., T.E. Schaffer, M. Viani, J.B. Thompson, N.A. Frederick, J. Kindt, A.
Belchers, G.D. Stucky, D.B. Morse, and P.K. Hansma. 1999. Molecular
Mechanistic Origin of   the Toughness of Natural Adhesives, Fibres, and
Composites. *Nature* 399:761-763.

Waite, J.H., and S.O. Anderson. 1978. 3,4-Dihydroxyphenylalanine in an Insoluble

Shell Protein of *Mytilus edulis*. *Biochem. Biophys. Acta* 541:107-114.

Waite, J.H. 1992. The DOPA Ephemera: A Recurrent Motif in Invertebrates. *Biol. Bull.*

183:178-184.

Wheeler, A.P., K.W. Rusenko, D.M. Swift, and C.S. Sikes. 1988. Regulation *of in*

vitro and *in vivo* CaCO$_3$ Crystallization by Fractions of Oyster Shell Organic

Matrix. *Mar. Biol.* 98:71-80.

Wheeler, A. P. 1992. Phosphoproteins of Oyster (Crassostrea Virginica) Shell Organic

Matrix. Hard Tissue Mineralization and Demineralization, 171-87, Springer,

New York.

Zhang, C., L. Xie, J. Huang, X. Liu, and R. Zhang. 2006. A Novel Matrix Protein

Family Participating in the Prismatic Layer Framework Formation of Pearl

Oyster, *Pinctada fucata. Biochem. Biophys. Res. Comm.* 344:735-740.

APPENDICES

Appendix 1: Protein Hydrolysis

What you will need –

> Refrigerated cold trap
> Aspirator
> 6-7 M HCl
> Trifluoroacetic aid
> Parafilm
> Propane
> Vacuum pump
> Condenser bulbs
> Molecular grade water and ethanol
> Amino Acid Analyzer
> Pipetman 100/200 microliter
> Safety shades
> Heating block
> Long stem Pasteur pipette
> Liquid phenol
> Long neck 1 mL hydrolysis vials
> Oxygen torch
> Oxygen with 2 stage regulator
> Vacuum gauge
> Cortex tubes
> NaS buffer
> Sample loops
> 10 mL beaker

Procedure for Hydrolysis of Hemolymph Samples:

1. Empty and dry the cold trap – reassemble properly such that the intake tubing is always in-line with the cold finger.
2. Turn on cold trap – Wait for frost to form on the insulated black coil tube of the refrigeration unit (30 min).
3. Turn on heating block. Be sure it is steady at 150°C.
4. Use an aspirator to vacuum dust out of the hydrolysis vials with long stem Pasteur pipette.
5. Pipette sample into vial followed by 10 microliters phenol, 100 microliters of 6M HCl, and 75 microliters sample.
6. Stretch Parafilm over vials. Poke hole through Parafilm with clean needle.
7. Once frost has formed, put your safety goggles on and light the torch:
   a. Propane supply is over the centrifuge in Cannon 119. Be sure lines are connected properly.
   b. Turn on main stage on the oxygen cylinder. Set second stage at 1.25 bar.
   c. Adjust red and green valves to give a good flame – about 4-5 cm long with very sharp tip.

8. Turn on vacuum pump. Allow vacuum to reach 70 μ.
9. Turn on pressure gauge.
10. Using your right hand, crimp the red rubber tubing, remove remains of previous vial, insert new vial, and slowly release the crimp in the tube.
11. Seal the vial by turning it evenly in the flame. When the glass is soft, pull away at the end connected to the rubber tubing. If you are doing a number of hydrolysates, you may wish to dip the hot end connected to the tubing into water before removing it. If you do so, do not forget to crimp the tubing.
12. When finished:
    a. Turn off the pump – immediately release pressure in the lines by removing the last vial from the red tubing, then put the vial back in the opening of the tubing.
    b. Turn off the pressure gauge.
    c. Turn off the cold trap.
    d. Turn off the gas and oxygen at their sources and then close the knurled red and green valves on the torch (Do not overtighten the valves).
13. Place the vials in the heating block overnight.

Appendix 2: Amino Acid Analysis Preparation and Loading

Preparation for Amino Acid Analysis:

1. Remove vials from heating rack (Allow to cool if necessary).
2. Crack vials at gold line indicated on the vial.
3. Transfer the entire sample into 1.5 mL centrifuge tubes.
4. Add 1 mL of DI water to the tubes as well.
5. Place the tubes (lids open and facing out) in the SpeedVac Concentrator for 4 hours on high heat setting.
6. Disassemble a BD 1 mL syringe. Place a serological filter on the end of the syringe.
7. Remove the samples from the centrifuge tubes using a Pasteur pipette and add them to the syringe.
8. Reassemble the syringe with sample inside and squeeze sample through the filter into analyzer vials.
9. Once sample is places through the filter, add water to the syringe and filter this into the analyzer vials as well. The total volume of liquid should be approximately 1 mL in each analyzer vial.

Loading the Amino Acid Analyzer:

1. Check buffer levels of 8 buffers in the front lower right of analyzer and two on the side. Check integrator paper supply (3 sheets are required for each cycle; a role has 200 sheets).
2. Follow steps 1-6 outlined on the analyzer.
3. Load samples:
    a. Take sample up in an appropriate amount of NaS buffer (final volume 40 microliters).
    b. Distribute an appropriate amount of sample along with two 30 microliter droplets of NaS per sample on a piece of Parafilm.
    c. Using the loading syringe and a clean coil, draw the buffer and sample into the coil. If you have never done this before, have someone show you. The correct order for loading a coil is:
        i. NaS buffer from a beaker until the buffer has reached 3 o'clock in the innermost forward lane.
        ii. Bubble
        iii. First 30 microliter droplet
        iv. Sample
        v. Bubble
        vi. Second 30 microliter droplet
        vii. Bubble
        viii. NaS buffer from a beaker until the front of the first bubble is at 9 o'clock in the second lane in from the edge.
4. Place the coal in the appropriate slot in the carousel of the analyzer.
5. Follow steps 7-9 of the instructions on the analyzer.
6. Log in carousel position, integrator number, sample ID, sample volume, date, name, and any buffer replacements.

Appendix 3: Standard Preparation and Amino Analyzer Buffer Preparation

Standards used for Amino Acid Analysis: 312, 625, 1250

	Amino Acid	L-DOPA	4-hydroxy	DI water
312	5 µL	7 µL	7 µL	975 µL
625	10 µL	14 µL	14 µL	949 µL
1250	20 µL	28 µL	28 µL	898 µL

Preparation of components used in Standards:

L-DOPA	4.93 mg L-DOPA, fill volumetric flask to 25mL with DI water
4-hydroxy	3.27 mg 4-hydroxy, fill volumetric flask to 25mL with DI water
OPS	4.63 mg OPS, fill volumetric flask to 25mL with DI water
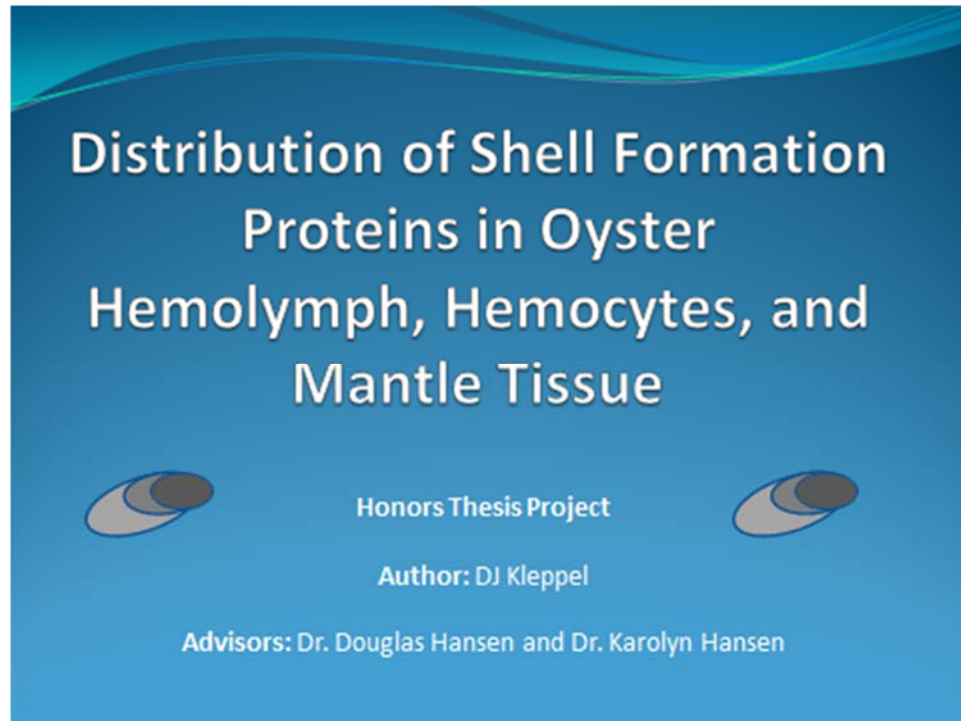
*Shake all samples well in capped volumetric flask once filled.

Amino Acid Analyzer Buffer Preparation:

A:	DI water	10mMNaOH / DI water	0.524 mL 50% NaOH to 1 L DI water vol.
B:	250 mM NaOH	13.1mL 50% NaOH	1 L DI water
C:	25mM NaOH + 1.0M NaCH3COO	1.3mL 50% NaOH + Na-Hac	1 L DI water

Any and all questions for amino acid analyzer preparation, loading, running, and analysis should be directed towards Christine Malloy/UDRI.

Appendix 4: University of Dayton Honors Symposium Presentation, March 4, 2016

Research: Focus

- Distribution and composition of L-DOPA proteins in oyster shell formation.

- Specific Aim #1: Determining the occurrence of L-DOPA biomarker in oyster hemolymph, hemocytes, mantle tissue, and newly formed shells.

- Specific Aim #2: Observing if there is a change in L-DOPA concentration as the oyster shell is repaired following a notching event.
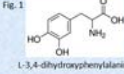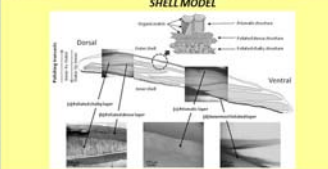

Materials & Methods

- Oysters obtained from Pemaquid Oyster Co., Waldoboro ME

Day 4: 96 hours

Week 2

Week 3

Week 4

12 Weeks of Repair
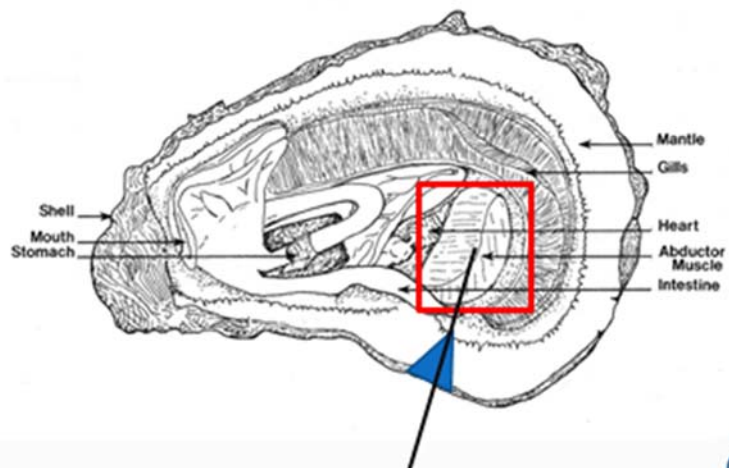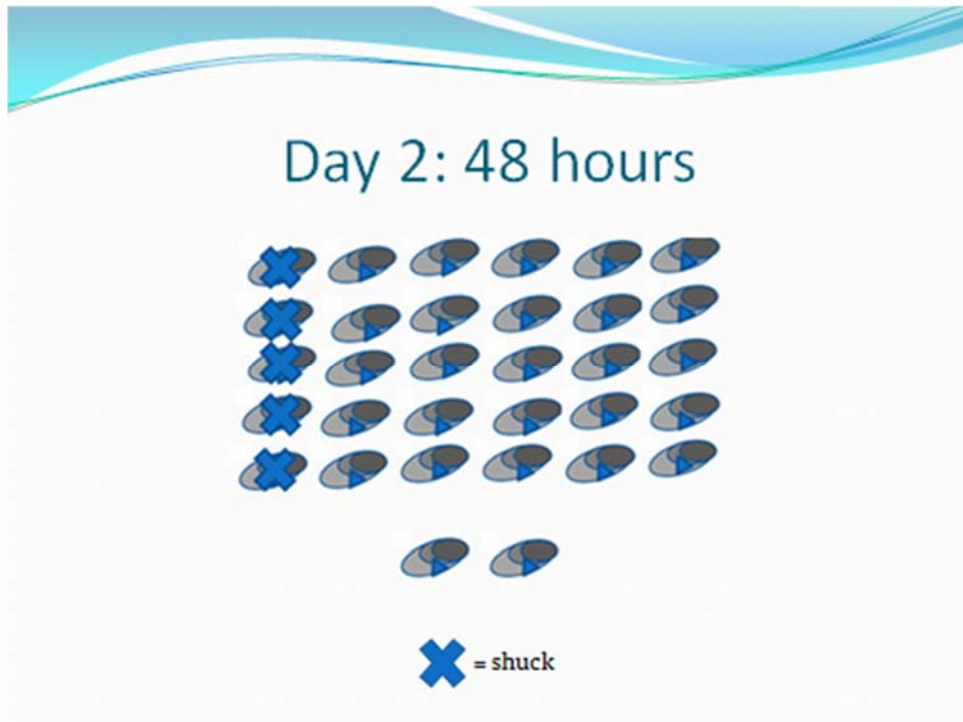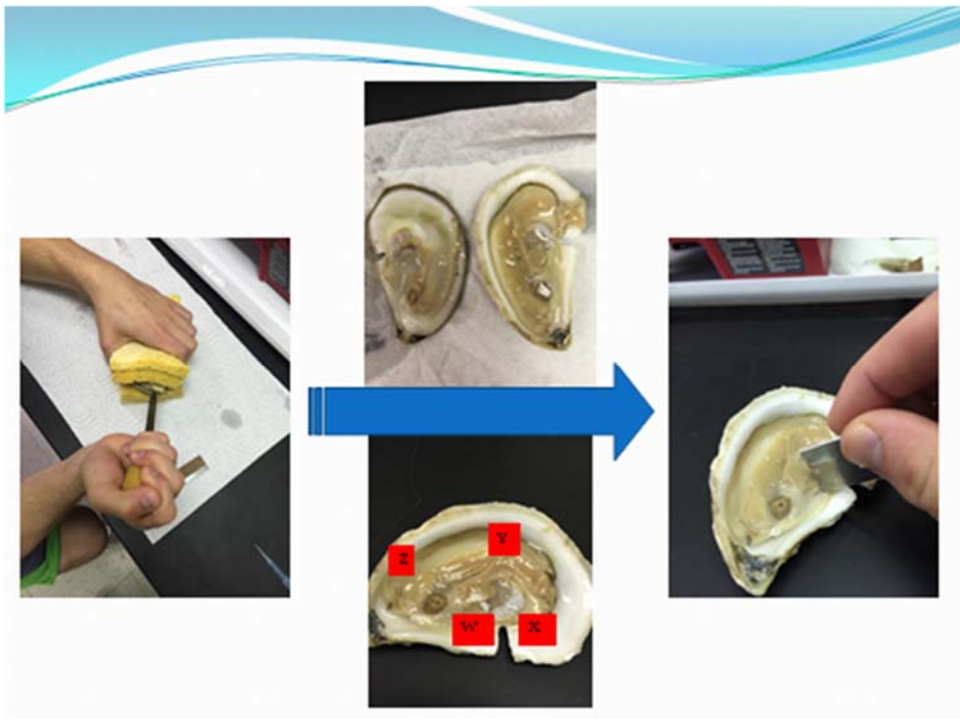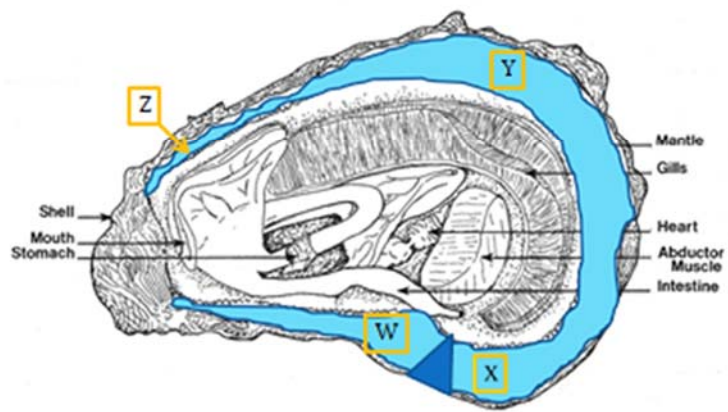
Sample Run Times

	cyte	lymph	mantle	new shell		
0 hr	32	32	0	0		
48 hr	5	5	20	0		
96 hr	5	5	20	0		
168 hr	5	5	20	0		
2 week	5	5	20	0		
3 week	5	5	20	5		
4 week	5	5	20	5		
total:	62	62	120	10		

Final:	254					

254 samples at 3 runs per sample at 80 minutes per run = 60,960 minutes

60,960 minutes = 1,016 hours = 42.3 days = 6.04 weeks

0 hr	3
48 hr	3
96 hr	3
168 hr	3
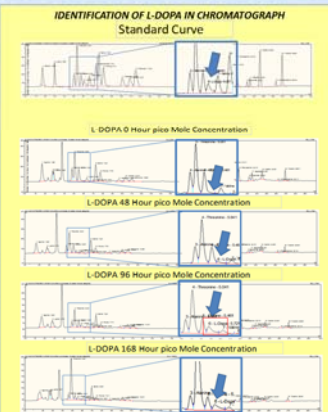
Samples: 12
48 hr total run time

Identification of L-DOPA in Chromatograph

L-DOPA 96 Hour pico Mole Concentration

L-DOPA 168 Hour pico Mole Concentration
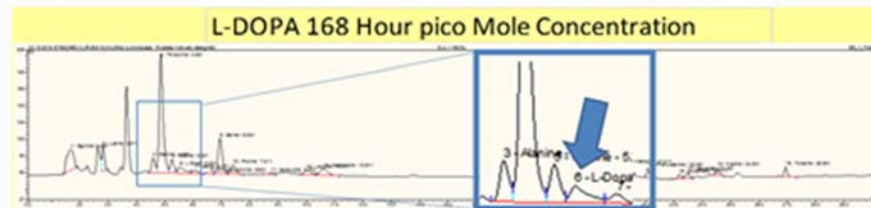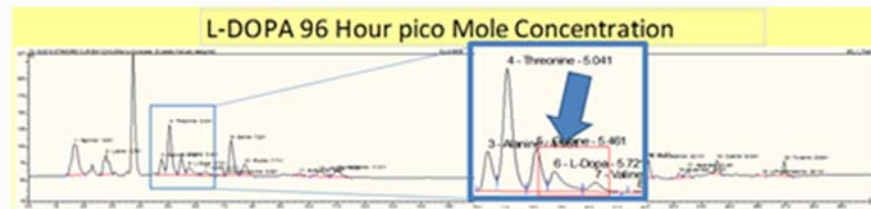
Results

Chromatograph Data Analysis pico Mole Concentration

	Avg. Mean	Avg. stdev	Avg. %RSD
0hr -	0	0	0
48hr -	159.182	36.45395	49.61977
96hr -	477.0401	21.08499	3.9536
168hr -	161.6811	4.149533	2.632845

Results

Concentration of L-DOPA in Week 1 Hemolymph
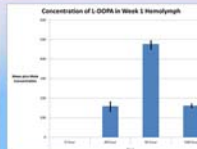
Mean pico Mole Concentration

600
500
400
300
200
100
0

O hour   48 hour   96 hour   168 hour
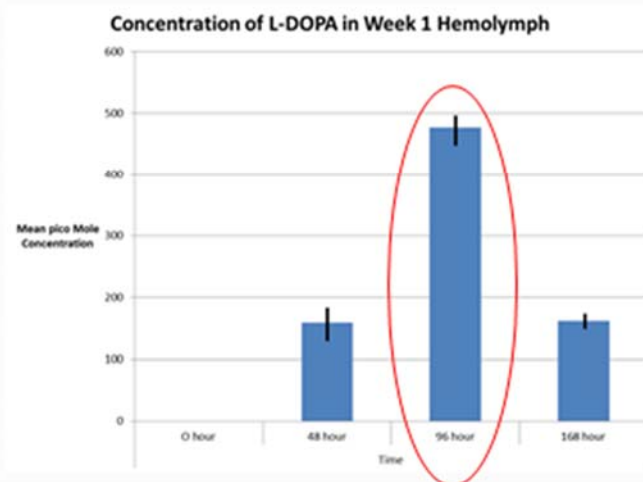
Time

Discussion

- Samples of hemolymph, hemocytes, mantle tissue, and newly regenerated shell obtained from all time points.
- Hemolymph at 0hr, 48hr, 96hr, and 168hr time points analyzed using amino acid analysis.
- Hemolymph sample results suggests that L-DOPA protein levels are rising in the days after notching has occurred.
- Spike in L-DOPA levels at the 96hr period suggests that there is a significant increase in pre-cursor protein allocation for shell repair.

Application

- Biomaterials application
  - Bone regeneration
  - Prosthetics = better interfaces
  - WPAFB UDRI →anticorrosion barrier coatings

- Global Warming & Ocean Acidification
  - Further insight into shell regeneration

Future Direction

- Process remaining hemolymph, hemocyte, mantle tissue, and repair shell samples to better determine how the oyster allocates protein resources for shell repair on a short time frame (immediate repair) and longer time frame (weeks after notch event).
- Take SEM images of shell repair

- *Journal of Shellfish Research*

- Ben Schmeusser continuation of research for future honors thesis
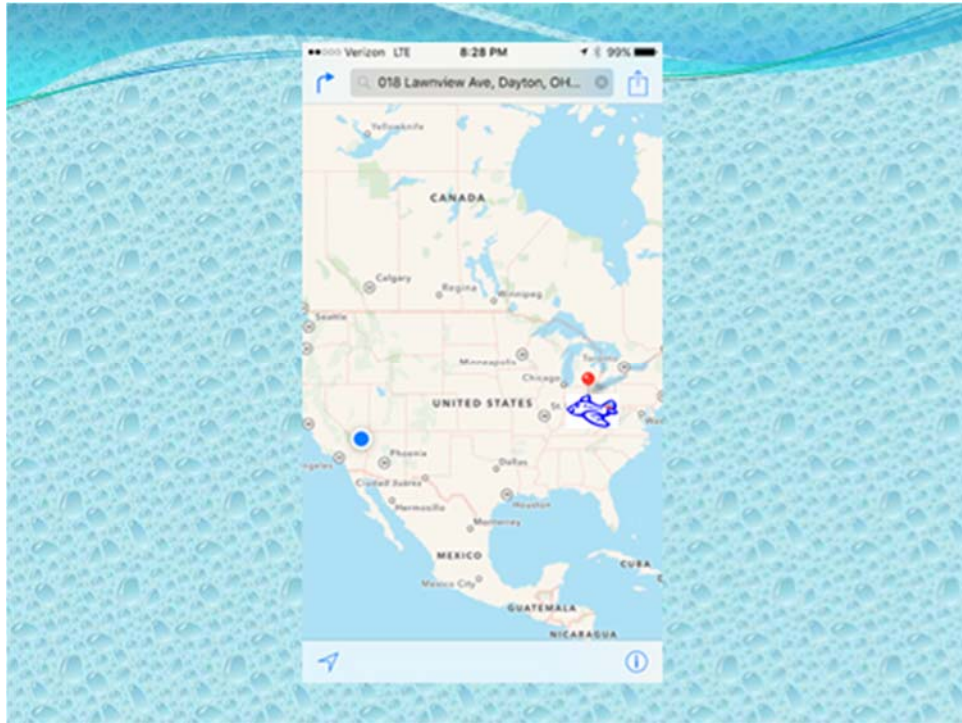
Acknowledgements

- University of Dayton Honors Program Funding
- Dr. Douglas Hansen and Dr. Karolyn Hansen (Advisors)
- University of Dayton Department of Biology, University of Dayton Research Institute
- Christine Malloy (Data Processing and Analysis)
- Benjamin Schmeusser (Undergraduate Assistant)

Questions / Comments
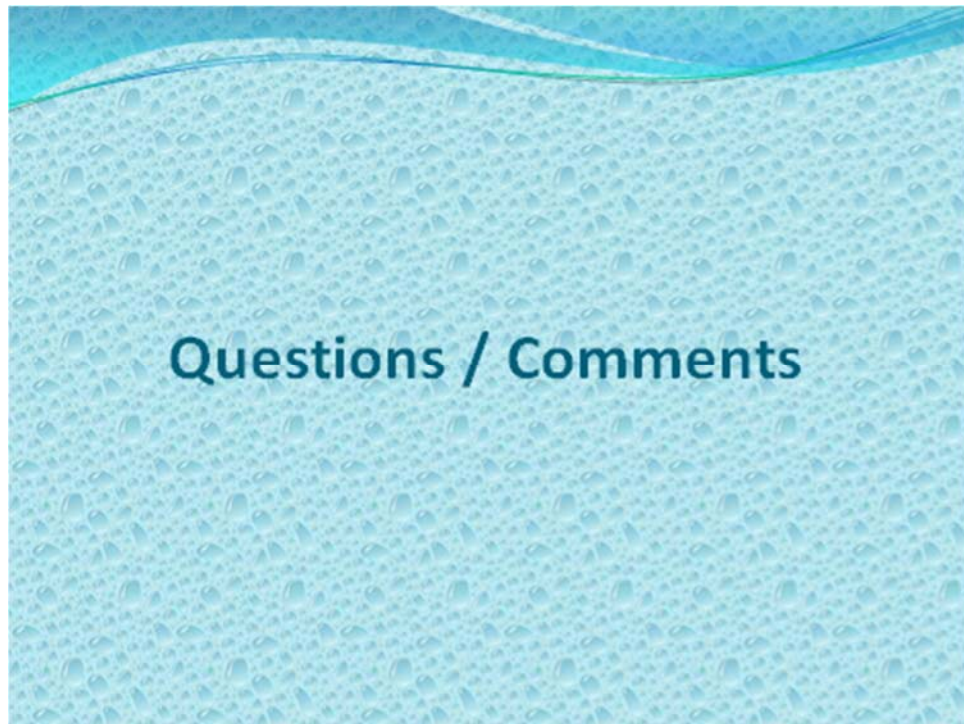
Appendix 5: Poster Presentation, National Shellfisheries Association Annual Meeting, February 2016, Las Vegas NV, USA